

## RESEARCH ARTICLE

View Article Online

View Journal | View Issue

Cite this: *Inorg. Chem. Front.*, 2021, **8**, 3491

# M/TiO<sub>2</sub> (M = Fe, Co, Ni, Cu, Zn) catalysts for photocatalytic hydrogen production under UV and visible light irradiation†

L. Díaz, <sup>a,b</sup> V. D. Rodríguez, <sup>\*c,b</sup> M. González-Rodríguez, <sup>a,b</sup>  
E. Rodríguez-Castellón, <sup>\*d</sup> M. Algarra, <sup>d</sup> P. Núñez <sup>a,b</sup> and E. Moretti<sup>e</sup>

In order to improve the photocatalytic response of TiO<sub>2</sub> to UV and visible light for hydrogen photoproduction, low cost M/TiO<sub>2</sub> semiconductor catalysts were prepared by the impregnation method of five different first row transition metals (M = Fe, Co, Ni, Cu or Zn) on a commercial titania support. The maximum hydrogen production efficiency was achieved for the Cu/TiO<sub>2</sub> photocatalyst, with ~5000 and ~220 μmol h<sup>-1</sup> g<sup>-1</sup> H<sub>2</sub> production rates for UV and visible irradiation, respectively. Ni/TiO<sub>2</sub> and Co/TiO<sub>2</sub> also showed a significant photocatalytic activity when UV light was used. The best performing catalyst, Cu/TiO<sub>2</sub>, was characterized by TEM and XPS measurements. The data showed that Cu was highly dispersed over the TiO<sub>2</sub> support and the copper species existed as both reduced Cu<sup>0</sup>/Cu<sup>+</sup> and oxidized Cu<sup>2+</sup> on TiO<sub>2</sub>. Besides, during the hydrogen production reaction, the reduced Cu was partially oxidized to Cu<sup>2+</sup> by the transfer of photogenerated holes under UV or visible light irradiation. With UV and visible lamps, the H<sub>2</sub> production rates were higher than those obtained with non-impregnated TiO<sub>2</sub> by factors of 16 and 3, respectively. These results demonstrated that a Cu/TiO<sub>2</sub> photocatalyst could be considered a promising low-cost alternative to the well-known Pt/TiO<sub>2</sub> system for hydrogen production, making the Cu-based catalyst an ideal cost-effective candidate for this reaction.

Received 31st October 2020,

Accepted 23rd May 2021

DOI: 10.1039/d0qi01311k

rsc.li/frontiers-inorganic

## Introduction

Minimizing environmentally harmful emissions and reducing the dependence on fossil fuels can be achieved by sustainable energy sources. Hydrogen can be an ideal sustainable energy carrier because it is readily available, has a high energy density and has a minimal environmental impact compared with fossil fuels.<sup>1,2</sup> Moreover, the storage capabilities, energy density versatility, transportability and environmental impacts of hydrogen are considered to be very important aspects in the assessment of its viability and use.<sup>3</sup> However, for hydrogen to become a common source of energy there need to be techno-

logical developments that facilitate the reduction of costs with innovative renewable hydrogen production methods.<sup>4</sup>

Hydrogen can be obtained from many different sources that include fossil resources, such as coal and natural gas, as well as renewable resources, such as biomass and water. Currently, the most developed and most used technology for hydrogen production is the reforming of hydrocarbon fuels. Nonetheless, to decrease the dependence on fossil fuels, several hydrogen generation technologies are being developed, including chemical, biological, electrolytic, photolytic, and thermo-chemical generation.<sup>5,6</sup>

Splitting water into hydrogen and oxygen could be the key technology in future hydrogen production. Photocatalytic water splitting is one of the most attractive methods since hydrogen can be produced from water and sunlight. In this regard, TiO<sub>2</sub> is the most used photocatalyst for hydrogen production from water. The main concern is the lack of photocatalytic activity under visible light irradiation. In fact, TiO<sub>2</sub> works only under UV light irradiation due to the wide band gap (3.2 eV for the anatase polymorph and 3.0 eV for the rutile one) and its photocatalytic performance is not sufficient for utilization since the amount of UV light contained in solar light is low (ca. 5%).<sup>7</sup> Consequently, many efforts have been devoted to the synthesis of photocatalysts responding to

<sup>a</sup>Departamento de Química, U.D. Química Inorgánica, Universidad de La Laguna, 38206 La Laguna, Tenerife, Spain

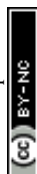
<sup>b</sup>Instituto Universitario de Materiales y Nanotecnología, Universidad de La Laguna, 38206 La Laguna, Tenerife, Spain

<sup>c</sup>Departamento de Física, Universidad de La Laguna, 38206 La Laguna, Tenerife, Spain. E-mail: vrguez@ull.edu.es

<sup>d</sup>Departamento de Química Inorgánica, Facultad de Ciencias, Universidad de Málaga, 29010 Málaga, Spain. E-mail: castellon@uma.es

<sup>e</sup>Dipartimento di Scienze Molecolari e Nanosistemi, Università Ca' Foscari Venezia, Via Torino 155, 30172 Mestre Venezia, Italy

†Electronic supplementary information (ESI) available. See DOI: 10.1039/d0qi01311k



visible light. Some research groups have reported that  $\text{TiO}_2$ -based photocatalysts modified with transition metal compounds on the surface respond to visible light.<sup>8–11</sup>

Certain metals, such as Pt, Au, Pd and Ag, can be deposited on  $\text{TiO}_2$  to increase the hydrogen production rate by photocatalysis, but these metals are expensive. Fig. 1 shows the scheme of the reaction of photocatalytic water splitting through irradiation of Pt/ $\text{TiO}_2$ . Photons are absorbed by the semiconductor-based photocatalyst to form electron-hole pairs. If the energy of the incident light is higher than the band gaps of the semiconductors, electrons and holes can be separated into the conduction (CB) and valence (VB) bands, respectively.

Photoexcited carriers are transferred to surface active sites and subsequently consumed by surface redox reactions; mass diffusion of reactants and products should concurrently proceed. Recombination of photoexcited carriers occurs along with these reactions. Hence, the charge separation in photocatalyst particles and the redox reactions on their surface must proceed within the lifetime of photoexcited carriers for successful water splitting.<sup>12,13</sup> However, the addition of organic compounds (alcohols, organic acids and azo-dyes) or biomass derivatives (glycerol and carbohydrates) as sacrificial reagents in the catalyst dissolution favours the photocatalytic activity. In this reforming process, the oxidation of organic molecules and the reduction of  $\text{H}^+$  to  $\text{H}_2$  occur. For example, when methanol is used as a sacrificial reagent, methanol photoreforming occurs ( $\text{CH}_3\text{OH} + \text{H}_2\text{O} \rightarrow 3\text{H}_2 + \text{CO}_2$ ), where  $\text{H}_2$  is obtained, and the sacrificial agents are mineralized.<sup>14,15</sup> However, most of these transition metal oxide-containing photocatalysts are generally found to remove contaminants from water.

Loading  $\text{TiO}_2$  with noble metals such as Pt, Pd or Au is an active research field for hydrogen production,<sup>16,17</sup> as it is an effective way to enhance the photocatalytic efficiency of  $\text{TiO}_2$  by reducing the fast recombination of photogenerated charge carriers. But unfortunately, it is unsuitable for large-scale energy production due to the high cost of the precious metals and their limited availability. Therefore, the modification of  $\text{TiO}_2$  with non-noble metals (Cr, Fe, Co, Ni, Cu, and Zn) could be a viable alternative, decreasing the band gap of  $\text{TiO}_2$  and extending the photoresponse range of the  $\text{TiO}_2$  matrix to the

visible region.<sup>18–22</sup> Different modification methods have been used over  $\text{TiO}_2$  with different phases, morphologies, and microstructures (as nanocrystals or nanofibers).

Recent experimental results have demonstrated that Cu is a good candidate to replace Pt as an efficient and cost-effective co-catalyst for  $\text{H}_2$  production. Copper species have been incorporated into  $\text{TiO}_2$  by many different methodologies, such as sol-gel, impregnation, microemulsion and electroless plating.<sup>23–26</sup> It is difficult to control the active species and their size during the synthesis and post treating processes, and thus, the optimal Cu loading amount can vary from one process to another, and the active species are still in discussion.<sup>27</sup> However, it was found that the hydrogen-through-copper production was increased with respect to bare  $\text{TiO}_2$  by a factor of 4.<sup>23</sup>

On the other hand, the efficiency reached is usually expressed in terms of the hydrogen generation rate by the mass unit of the catalyst. But this rate depends on the experimental setup and cannot be used to compare the results obtained by different authors for different photocatalysts. In this sense, we consider it useful to compare the experimental results obtained with a new photocatalyst with those obtained with a well-known commercial one, such as  $\text{TiO}_2$  P25 from Degussa. Moreover, some authors present the results in terms of the obtained quantum yield, which is given by the ratio of hydrogen generated ( $2 \times$  hydrogen molecules) to the number of incident photons. Thus, Montoya *et al.* obtained a quantum efficiency of 0.4% for  $\text{TiO}_2$  P25 by using a 450 W Hg lamp.<sup>19</sup> This parameter depends on the experimental setup, the lamp spectrum, *etc.* Therefore, it is not useful to compare the results of different authors.

In a previous paper, we modified  $\text{TiO}_2$  nanoparticles by photodeposition of different percentages of Pt to obtain the best performance for hydrogen production. The effects of the reaction temperature and the sacrificial reagent (methanol, ethanol, or isopropanol) on the photocatalytic activity of Pt/ $\text{TiO}_2$  were also studied.<sup>28</sup> In this work, a series of M/ $\text{TiO}_2$  photocatalysts (M = Fe, Co, Ni, Cu and Zn) were prepared by an impregnation method to improve the photoresponse of  $\text{TiO}_2$  to UV and visible radiation for hydrogen photoproduction and also by replacing noble metal co-catalysts, such as Pt, which are relatively scarce and very expensive. In this sense, Earth-abundant elements, such as the proposed transition metals, could be appropriate alternatives if they show reasonable photocatalytic activity. The results obtained with  $\text{TiO}_2$  P25 by using the same experimental setup are presented as a reference of the accomplished efficiency. Moreover, the results for Pt/ $\text{TiO}_2$  obtained with the same experimental setup are also presented for comparison purposes.

## Results and discussion

### Influence of the transition metals supported on $\text{TiO}_2$

Traditionally, noble metal nanoparticles (Pt, Pd, Au, Rh, and Ag) have been used as cocatalysts in the photoreforming

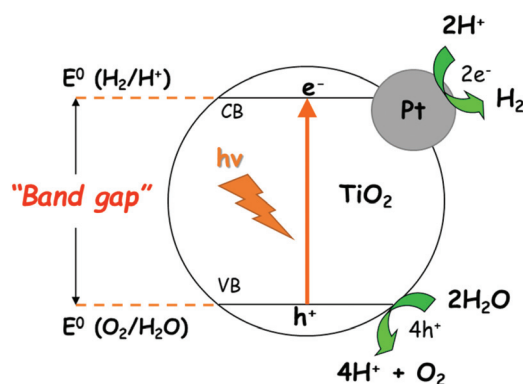


Fig. 1 Schematic diagram of the water-splitting reaction on Pt/ $\text{TiO}_2$  as a heterogeneous photocatalyst.



process for  $H_2$  production. It is well known that the presence of a cocatalyst can enhance photoactivity, providing additional reaction sites and favouring charge migration and separation. The latter promotional effect can be related to the formation of a Schottky barrier originating from the difference in the Fermi levels between the metal nanoparticles and the semiconductor (*i.e.*  $TiO_2$ ). This allows the injection of photogenerated electrons from the conduction band of the semiconductor into the metal.<sup>29</sup> Until now, few studies on the use of non-noble metals as cocatalysts have been reported.<sup>30–33</sup> To analyse the photocatalytic behaviour of the prepared  $M/TiO_2$  photocatalysts ( $M = Fe, Co, Ni, Cu$ , and  $Zn$ ) under both visible and UV light irradiation,  $TiO_2$  was loaded with 2 wt% of selected transition metals.

Hydrogen production profiles for  $TiO_2$  impregnated catalysts are shown in Fig. 2 and compared with the  $TiO_2$  P25 photocatalyst, without impregnation, using in both cases the same reactor system and the same operating conditions. As expected, bare titania did not show any remarkable activity, neither under UV nor under visible light irradiation. Overall, these impregnated photocatalysts presented a better photocatalytic activity for hydrogen production under UV light than that observed under visible light. As shown in Fig. 2, when UV light was employed, the highest hydrogen production was obtained for  $Cu/TiO_2$ , followed by  $Ni/TiO_2$  and  $Co/TiO_2$ , which showed much higher  $H_2$  production than the bare  $TiO_2$ . However,  $Fe/TiO_2$  and  $Zn/TiO_2$  showed a very poor photocatalytic activity, even lower than that displayed by pure  $TiO_2$ .

When visible light was used,  $Cu/TiO_2$  emerged again as the system providing the best photocatalytic activity (Fig. 3). The  $H_2$  production obtained with this material is about three times higher than that obtained with bare  $TiO_2$ . Conversely, the materials impregnated with  $Ni, Co, Zn$  and  $Fe$  exhibited lower hydrogen production than the pure  $TiO_2$ . Broadly, the  $Cu/TiO_2$  photocatalyst showed the best performance for hydrogen production, under both UV and visible light irradiation, achieving hydrogen production rates of  $5000$  and  $220 \mu mol h^{-1} g^{-1}$ , respectively.



**Fig. 2** Hydrogen production for impregnated  $M/TiO_2$  photocatalysts ( $M = Fe, Co, Ni, Cu, Zn$ ), 2 wt%  $M$ , under both visible and UV light irradiation.

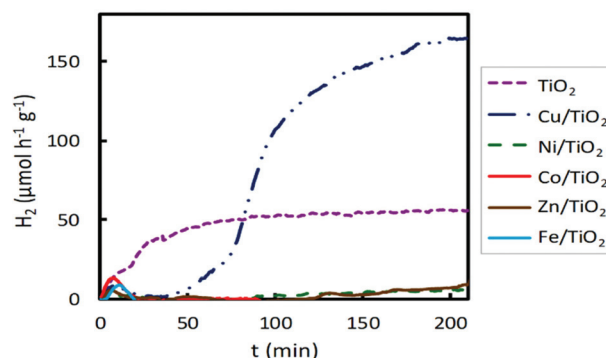


**Fig. 3** Hydrogen production for 2 wt% impregnated  $M/TiO_2$  photocatalysts ( $M = Fe, Co, Ni, Cu, Zn$ ) under visible lamp irradiation.

With both lamps, UV and visible, these  $H_2$  production rates are higher than those obtained with non-impregnated  $TiO_2$  by factors of 16 and 3, respectively. Furthermore,  $H_2$  production rates using UV light with  $Ni/TiO_2$  and  $Co/TiO_2$  photocatalysts were also high, see Fig. 2, achieving values of  $2300 \mu mol h^{-1} g^{-1}$  and  $2250 \mu mol h^{-1} g^{-1}$ , respectively.

#### Effect of Cu loading on $TiO_2$

The effect of the Cu content impregnated on the  $TiO_2$  matrix was examined by varying the percentage of Cu between 0.1 and 9 wt% to identify the optimal loading of the best performing cocatalyst. Usually there is an optimum cocatalyst loading towards enhanced photoactivity which varies depending on the cocatalyst used. Catalytic activity, in the beginning, increases with increasing cocatalyst amount on the surface of the semiconductor support.

Then a further increase in the cocatalyst loading normally results in a decrease in the overall photocatalytic activity. This fact has been attributed both to shading effects, caused by the excess cocatalyst loading, and to an increase of the particle size with increasing cocatalyst content, with detrimental effects in charge recombination and specific surface area.<sup>34</sup>

The results obtained for hydrogen production under UV irradiation over Cu-based photocatalysts are shown in Fig. 4. As reported before, bare  $TiO_2$  presents an extremely low hydrogen production, which is limited by the rapid recombination of the photogenerated electron-hole pairs. When a small amount of copper, 0.1 wt%, was loaded on the semiconductor surface, a significant improvement in photocatalytic activity was achieved. The increase in the Cu content, from 0.1 to 0.5 wt%, resulted in a remarkable enhancement in hydrogen production. Then, between 0.5 and 3.0 wt% of Cu content, hydrogen production for these Cu loadings is possibly due to the fact that the active sites on the  $TiO_2$  are sufficient and the cocatalyst can trap the photogenerated charges and assist in the charge separation appropriately. However, a further increase in the Cu content beyond 3 wt% (namely, 6.0 and 9.0 wt%) led to a decrease in the hydrogen production, probably due to several combined effects: (a) the percolation effects are over, that is, the active sites on the  $TiO_2$  surface begin to



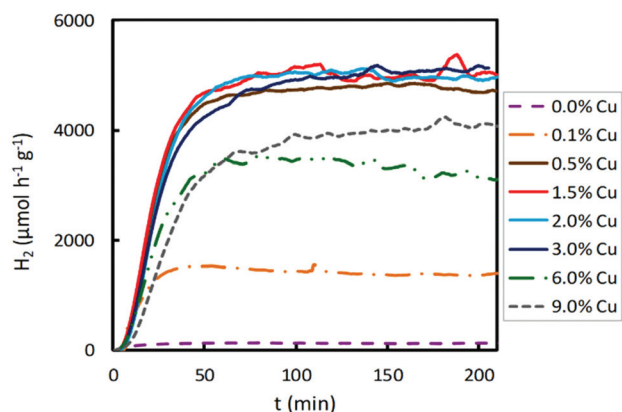


Fig. 4 Effect of Cu content on photocatalytic hydrogen production under UV light irradiation.

decrease because they are highly occupied by the Cu species, and (b) opacity and light scattering by the excessive Cu species agglomeration result in a decreased passage of irradiation.<sup>35,36</sup> Therefore, when UV irradiation was employed for photocatalytic hydrogen production, the optimum Cu content on TiO<sub>2</sub> was in the range of 0.5–3.0 wt%, achieving the highest hydrogen production (4700–5100  $\mu\text{mol h}^{-1} \text{g}^{-1}$ ).

The effect of the Cu content of Cu/TiO<sub>2</sub> samples on photocatalytic hydrogen production using visible light was also studied. The results are presented in Fig. 5. The hydrogen production was two-fold when TiO<sub>2</sub> was impregnated with 0.1 wt% Cu. When the Cu content was increased from 0.1 to 1.5 wt%, the hydrogen production enhanced, achieving a maximum production for a Cu content of 1.5 wt%. For a copper loading higher than 1.5 wt%, the photocatalytic activity decreased. With higher Cu contents, from 1.5 to 9.0 wt%, lower H<sub>2</sub> production was obtained. As discussed above, an excessive titania coverage by copper did not improve the ability of TiO<sub>2</sub> to photogenerate hydrogen since a too large amount of Cu species led to agglomeration on the semiconductor

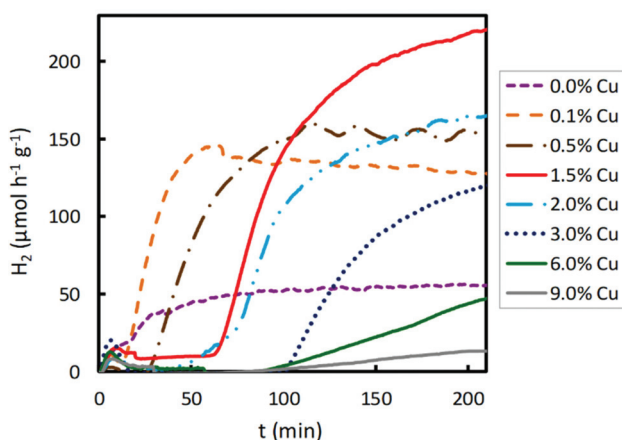


Fig. 5 Effect of Cu impregnated content of TiO<sub>2</sub> on photocatalytic hydrogen production under visible light irradiation.

surface, decreasing the light absorption of TiO<sub>2</sub> and partially blocking its sensitization.<sup>37</sup> Furthermore, it is known that excessive metal sites may act as recombination centres.<sup>38</sup> Consequently, when visible light was used for the photocatalytic hydrogen production, the optimum Cu content was 1.5 wt%, achieving the highest hydrogen production of about 220  $\mu\text{mol h}^{-1} \text{g}^{-1}$ , a value much lower than that obtained under UV light.

A noticeable delay of H<sub>2</sub> production onset in Cu impregnated TiO<sub>2</sub> compared to bare TiO<sub>2</sub> is observed in Fig. 4 and 6, which increases with the Cu content. This delay could be associated with an initial photoreaction caused by the visible lamp, which is not appreciable with the UV lamp. Also, in Fig. 2, Co impregnated TiO<sub>2</sub> shows delay under the UV lamp.

In Fig. S1† it is clear that 1.5% of the Cu sample shows the highest hydrogen production under visible light irradiation, and that high Cu contents (6.0 and 9.0%) give rise to low hydrogen production, even lower than the pristine support, as explained above. Under ultraviolet irradiation, samples with medium Cu contents (0.5, 1.0, 2.0 and 3.0%) show similar high hydrogen productivity; however, higher Cu contents (6.0 and 9.0%) give rise to lower productivity.

As mentioned earlier, Pt is the most efficient cocatalyst on TiO<sub>2</sub> for photocatalytic hydrogen production. For this reason, comparative studies of the hydrogen production rate under UV irradiation of 2.0 wt% Cu or Pt impregnated TiO<sub>2</sub> were performed. The obtained results are shown in Fig. 6. The Pt-TiO<sub>2</sub> photocatalyst was prepared by photodeposition, following the procedure proposed by several authors.<sup>39,40</sup> The highest catalytic activity was obtained for Pt/TiO<sub>2</sub>; however, Cu/TiO<sub>2</sub> achieved ~80% of the H<sub>2</sub> production rate of Pt/TiO<sub>2</sub>. This fact suggests the great potential of the Cu/TiO<sub>2</sub> photocatalyst in hydrogen production if the metal prices are compared.<sup>41</sup>

### Cu/TiO<sub>2</sub> characterization

The TEM images of 2 wt% Cu/TiO<sub>2</sub> and 9 wt% Cu/TiO<sub>2</sub> samples, chosen for a comparative study, are very similar, as

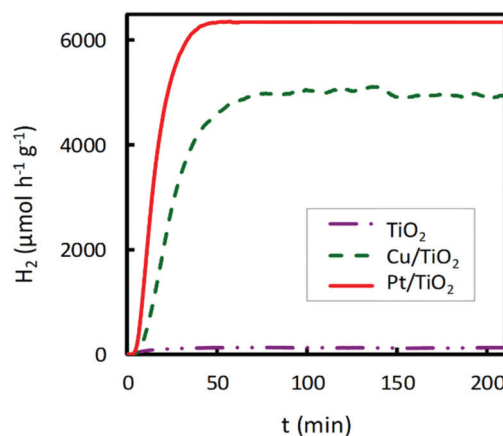
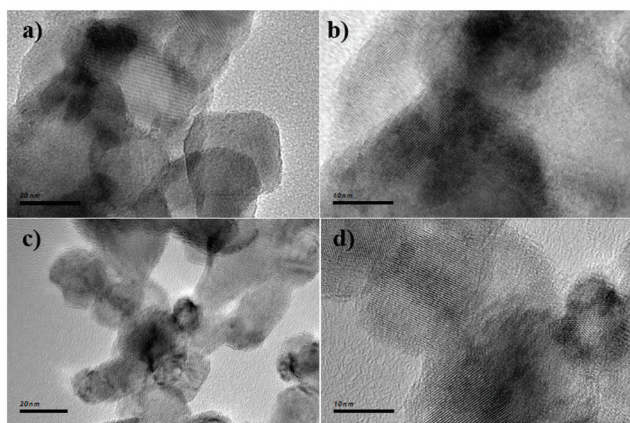


Fig. 6 Comparison of the catalytic activity of bare commercial TiO<sub>2</sub>, 2 wt% Cu/TiO<sub>2</sub> and 2 wt% Pt/TiO<sub>2</sub> in the hydrogen photoproduction under UV irradiation.







**Fig. 7** TEM images of the Cu/TiO<sub>2</sub> photocatalysts: (a and b) 2 wt% Cu and (c and d) 9 wt% Cu.

shown in Fig. 7. They show the starting TiO<sub>2</sub> crystalline nanoparticles, without evidence of Cu-associated nanoparticles. The clear lattice fringes indicate the crystallinity of the samples and a *d*-spacing of 0.35 nm in all TEM images, in agreement with that of the (101) plane of anatase TiO<sub>2</sub>.<sup>42</sup> The lack of nanoparticles corresponding to the agglomeration of Cu species observed from the TEM images confirms the high dispersion of Cu species on the titania surface. EDX analysis of both Cu/TiO<sub>2</sub> systems shows two strong fluorescence signals (Fig. 8a and c), indicating the presence of Cu species. In addition, to clarify the distribution of the Cu species on the TiO<sub>2</sub> surface, X-ray elemental mapping analysis was carried out, as shown in Fig. 8b and d. These figures show that the spatial distribution of Cu is in good agreement with the O and Ti mappings, confirming that the Cu species are highly dispersed on the surface of TiO<sub>2</sub><sup>43</sup> according to that reported by Chen *et al.*,<sup>44</sup> who prepared a CuO/TiO<sub>2</sub> system by a complex precipitation method and suggested that a CuO monolayer was deposited on the titania surface. Under these conditions, electron diffraction, carried out in the HRTEM equipment, does not reveal the presence of the Cu species, which are localized as thin films over TiO<sub>2</sub> nanoparticles.

The chemical states of Ti and Cu elements on the TiO<sub>2</sub> surface were analysed by X-ray photoelectron spectroscopy (XPS). Two catalytic materials were studied before the photocatalytic reaction: 2 and 9 wt% Cu/TiO<sub>2</sub>; the latter was also studied after the reaction. For this purpose, the material was separated from the reaction medium by centrifugation and then dried for 24 hours in air at room temperature. As shown in Fig. 9, all the catalysts show the characteristic doublet Ti 2p<sub>3/2</sub> and Ti 2p<sub>1/2</sub> at binding energies of 458.7 and 464.3 eV, respectively, revealing that titanium atoms exist as Ti<sup>4+</sup> in the lattice of TiO<sub>2</sub>.<sup>45,46</sup> No significant variation was observed between the Ti 2p binding energies of TiO<sub>2</sub> and Cu/TiO<sub>2</sub> catalysts, indicating the Cu was deposited on the TiO<sub>2</sub> surface rather than being incorporated into the TiO<sub>2</sub> lattice.<sup>46</sup> Furthermore, the Cu 2p core level spectra of these materials are shown in Fig. 10.

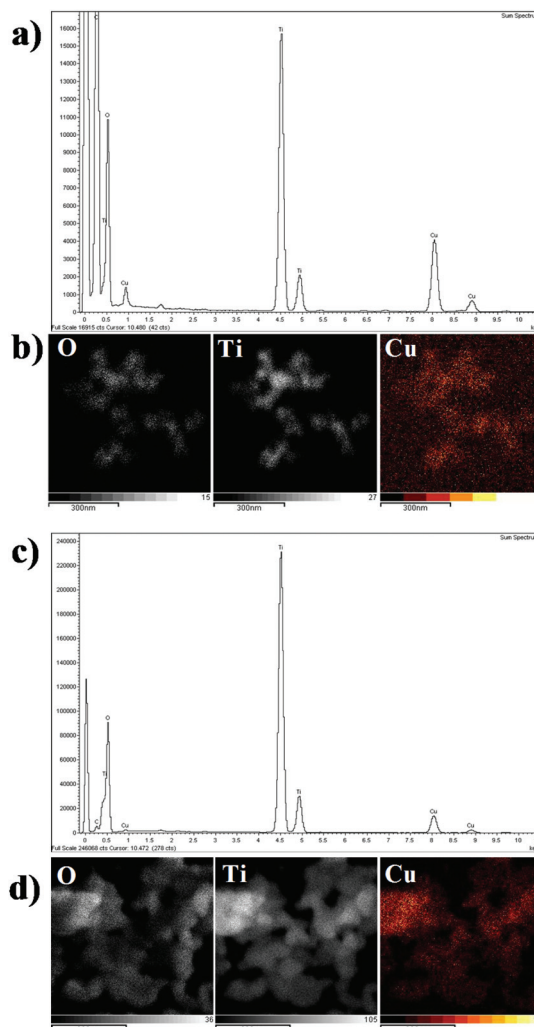


**Fig. 8** EDX analysis of (a) 2 wt% Cu/TiO<sub>2</sub> and (c) 9 wt% Cu/TiO<sub>2</sub> element mapping of O, Ti and Cu for (b) 2 wt% Cu/TiO<sub>2</sub> and (d) 9 wt% Cu/TiO<sub>2</sub>.

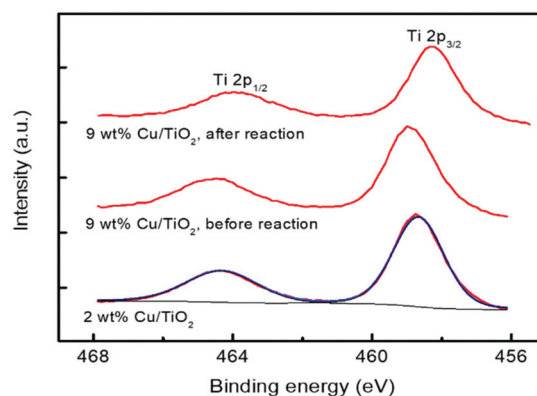


**Fig. 9** XPS spectra of Cu 2p for 2 wt% and 9 wt% Cu/TiO<sub>2</sub> samples.

The two catalysts present two peaks at 932.7 and 952.5 eV, both of them corresponding to reduced Cu<sup>0</sup>/Cu<sup>+</sup>, together with peaks at 935.0 and 954.9 eV (main peaks) and 941.5, 944.0 and 962.2 eV (satellites) due to Cu<sup>2+</sup>.<sup>47,48</sup>



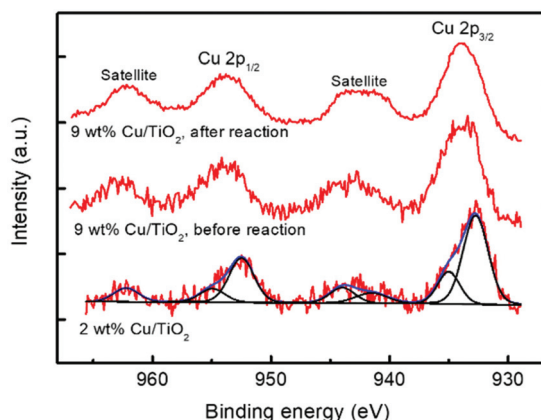


**Fig. 10** XPS spectra of Cu 2p for 2 wt% and 9 wt% Cu/TiO<sub>2</sub> samples. Deconvolution into the main and satellite peaks is shown.

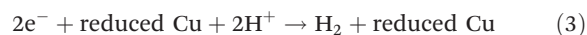
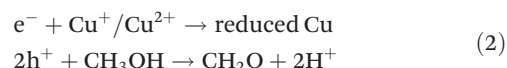
The deconvolution into these peaks for the 2% Cu/TiO<sub>2</sub> spectrum is shown in Fig. 10. The ratios of reduced to oxidized Cu are 1.6 and 0.7 for 2.0 and 9.0 wt% Cu/TiO<sub>2</sub>, respectively, and the last one decreases to 0.4 after the reaction. These results indicate that Cu is partially oxidized from the reduced Cu species to Cu<sup>2+</sup> by the photocatalytic reaction. Short irradiation times were used when acquiring the Cu 2p spectra to avoid the photoreduction of the Cu species. For this reason, the Cu LMM signal is very noisy and the assigning of the oxidation state for the reduced copper species is not possible. The XPS spectra provide us with very valuable information since the characterization of the surface confirms the simultaneous presence of Cu<sup>+</sup>/Cu<sup>2+</sup> species. The existence of these two species on the surface of the samples suggests that anionic vacancies are generated.

These vacancies could generate electronic gaps, which could determine the separation of charges, allowing greater methanol degradation with respect to the bare TiO<sub>2</sub>.

The Cu metal and Cu<sub>2</sub>O semiconductor have been reported as enhancers of the H<sub>2</sub> production on TiO<sub>2</sub> nanoparticles.<sup>24,47,49</sup> These species are present in the catalysts investigated before the photocatalytic reaction and could be responsible for the large increase of the H<sub>2</sub> production observed in our Cu/TiO<sub>2</sub> catalysts, with respect to the bare TiO<sub>2</sub>. However, different authors have proposed that CuO clusters also increase the H<sub>2</sub> production on TiO<sub>2</sub>.<sup>44,48</sup> Therefore, the observed CuO clusters, which are enlarged by the photocatalytic reaction, could also contribute to the increased H<sub>2</sub> production. CuO and Cu<sub>2</sub>O present band gaps, of 1.3 and 2.1 eV, shorter than TiO<sub>2</sub>, which lead to absorption at 950 and 590 nm, respectively.

Therefore, these semiconductors present absorption of visible light. Moreover, metallic Cu nanoparticles also present absorption in the visible range associated with surface plasmon resonance. Visible absorption by the different species of copper present on the samples would be responsible for the observed enhancement of the visible-light photoactivity.

The possible mechanisms for the redox reactions with photoreforming are as follows:<sup>19</sup>



The band gaps obtained for different Cu-containing tested materials are shown in Table 1. These were determined from the UV-Vis diffuse reflectance spectra (Fig. S2 and S3†).

The impregnation of the TiO<sub>2</sub> structure with the Cu species led to the reduction of the band gap, achieving a lower value of 3.03 eV for the sample with 0.5 wt% of Cu.

In Fig. 11, a comparison of the photoluminescence spectra of bare titania and Cu/TiO<sub>2</sub> photocatalysts with copper loadings of 2 and 9 wt% is reported. After irradiation at 340 nm, it is observed that the material displays a broad emission band centered at *ca.* 420 nm, regardless of whether the system contains Cu or not (Fig. 11). This level identified as Fermi level, which did not show any shift for doping effect, with an energy of 2.952 eV, was observed in the size control of Cu nanoparticles (Fig. 7).<sup>50</sup> It can be noticed that when the Cu concen-

**Table 1** Band gaps of the studied copper-containing catalysts and of the pristine P25 support

Cu/TiO <sub>2</sub>	Band gap (eV)
P25	3.20
P25-Cu0.1	3.12
P25-Cu0.5	3.03
P25-Cu1.5	3.05
P25-Cu2	3.10
P25-Cu3	3.05
P25-Cu6	3.14
P25-Cu9	3.16

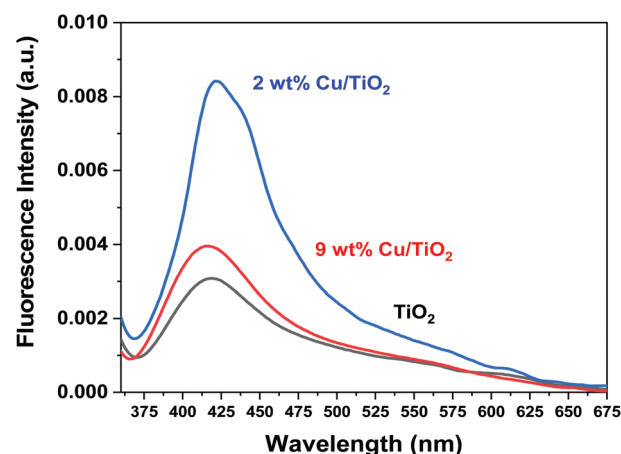


**Fig. 11** Photoluminescence spectra of the obtained bare TiO<sub>2</sub> and titania modified with Cu (2 and 9 wt%), when excited at 340 nm.



tration is optimized at 2 wt%, the Fermi level shows higher energy as evidenced by the very intense band in terms of fluorescence emission, which can be converted into electrons photogeneration for higher H<sub>2</sub> production.

It has been reported in the literature that the hydrogen photoproduction using copper-based systems is strongly affected by the complex structural, morphological, and chemical features of copper species<sup>26</sup> and that the occurrence of the highly dispersed Cu<sup>+</sup>/Cu<sup>2+</sup> species is directly related to the higher performance of the system for the H<sub>2</sub> production reaction.<sup>51,52</sup>

In our work, it seems that, in the 2 wt% Cu/TiO<sub>2</sub> sample, both the optical properties and the structural-chemical properties contribute to enhancing the photocatalytic activity. This copper loading, besides displaying a much higher fluorescence band than the 9 wt% Cu/TiO<sub>2</sub> sample, is also advantageous for the investigated reaction since an excessive coverage of the titania surface by the active phase has detrimental effects on the ability of TiO<sub>2</sub> to photogenerate hydrogen. In fact, a too large amount of copper species could decrease the light absorption ability of TiO<sub>2</sub> and partially block its sensitization.<sup>37</sup> This, together with the fact that an excessive amount of metal particles may act as recombination centers,<sup>38</sup> makes the sample containing 2 wt% of copper the most suitable system for hydrogen photogeneration under UV light irradiation.

## Experimental

### Preparation of M/TiO<sub>2</sub> photocatalysts

M/TiO<sub>2</sub> (M = Fe, Co, Ni, Cu, Zn) catalysts were prepared by the impregnation method. In a typical synthesis, a suitable amount of the M precursor of Fe(NO<sub>3</sub>)<sub>3</sub>·9H<sub>2</sub>O (≥98%), Co(NO<sub>3</sub>)<sub>2</sub>·6H<sub>2</sub>O (≥98%), Ni(NO<sub>3</sub>)<sub>2</sub>·6H<sub>2</sub>O (99.999%), Cu(NO<sub>3</sub>)<sub>2</sub>·3H<sub>2</sub>O (≥99%) and Zn(NO<sub>3</sub>)<sub>2</sub>·6H<sub>2</sub>O (98%), supplied by Sigma-Aldrich, was used without further purification. To obtain 2.0 wt%, the nitrate metal loading was weighed and dissolved in ethanol (1.0 mL). As for copper, the loading was varied between 0.1 and 9.0 wt%. Each one of these solutions was well mixed with 0.3 g of the solid photocatalyst titanium dioxide (Degussa P25 TiO<sub>2</sub>), composed of rutile 20 wt% and anatase 80 wt%. As a result, a paste was formed, which was dried in an oven at 70 °C for 1 h and calcined at 350 °C for 8 h in a box furnace. Pt/TiO<sub>2</sub>, used for comparison purposes, was prepared as previously reported.<sup>28</sup>

### Photocatalytic hydrogen production

Photocatalytic experiments for hydrogen production were carried out in a novel and innovative confocal homemade system (Fig. 12). The reactor and lamps are located at the focus of an elliptic cylinder polished stainless-steel reflector. In this way, all the light coming from the lamp is reflected towards another focus, where the reactor is placed, achieving maximum radiation on the reactor. The reactor has a borosilicate double wall, which allows controlling the photocatalyst temperature by water circulation from a thermostatic bath. This setup includes two lamps: a UV lamp (Philips, HPA

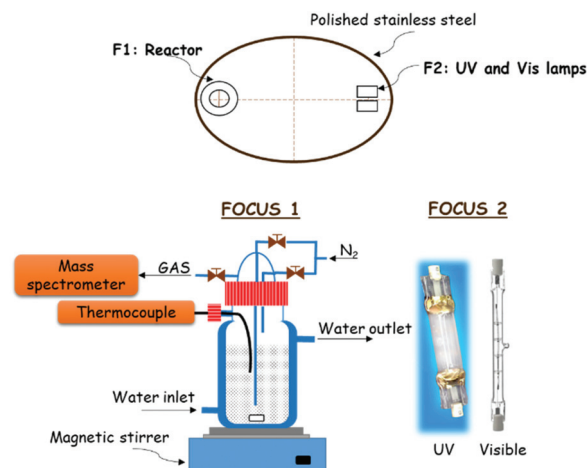


**Fig. 12** Scheme of the reaction system used for photocatalytic hydrogen production under UV and visible light irradiation at room temperature (20 °C) and atmospheric pressure.

Synergy 300 W) and a visible lamp (Leuci, Classic Linear Halogen, 500 W), which can be switched on independently. A fan blade was placed beside the lamps to prevent overheating. In a typical photocatalytic experiment, 150 mL of water and 50 mL of MeOH (25 vol%), as a sacrificial reagent, were added into the reactor equipped with magnetic stirring. Besides, 0.2 g of photocatalyst were also added to study its efficiency for hydrogen production. The reactor temperature was fixed at 20 °C by a continuous water flux through the reactor jacket during the experiment.

A continuous nitrogen flux of 13.2 mL min<sup>-1</sup> through the reactor was fixed by a mass flow controller (Bronkhorst, EL-FLOW Select). For dynamical measurements of hydrogen production, a mass spectrometer Omnistar of Pfeiffer Vacuum Co. (Aßlar, Germany) was used that was connected in line with the reactor.

### Characterization of Cu/TiO<sub>2</sub> photocatalysts

The morphology of Cu/TiO<sub>2</sub> photocatalysts was characterized using a transmission electron microscope (TEM 200 kV, Jeol JEM 2100). Prior to the measurement, the samples were dispersed in absolute ethanol followed by ultrasonication for 15 min. Then a drop of the resulting dispersion was placed on holey carbon coated copper TEM grids for analysis. XPS studies were carried out on a physical electronics spectrometer (PHI Versa Probe II Scanning XPS Microprobe) with monochromatic X-ray Al Kα radiation (100 μm, 100 W, 20 kV, 1486.6 eV) and a dual beam charge neutralizer. The spectrometer was calibrated using Cu 2p<sub>3/2</sub>, Ag 3d<sub>5/2</sub>, and Au 4f<sub>7/2</sub> photoelectron lines at 932.7, 368.2 and 84.0 eV, respectively. Under a pass energy of 23.5 eV, the Au 4f<sub>7/2</sub> line was recorded with 0.73 eV FWHM at a binding energy (BE) of 84.0 eV. The multiregion spectra were referenced with the C 1s signal of adventitious carbon at 284.8 eV. The recorded spectra were always fitted using Gauss–Lorentz curves. The atomic concentration percentages of the characteristic elements of the surfaces were determined considering the





corresponding area sensitivity factor for the different measured spectral regions. Photoluminescence spectra were obtained by excitation of the TiO<sub>2</sub> tablets with light from a 300 W Xe lamp passed through a 0.25 m double grating Spex monochromator. Fluorescence was detected using a 0.25 m Spex monochromator with a Hamamatsu R928 photomultiplier.

## Conclusions

M/TiO<sub>2</sub> modified-photocatalysts (where M = Fe, Co, Ni, Cu and Zn) were prepared by an impregnation method in order to replace the expensive noble metals with other cheaper transition metals for hydrogen production under both UV and visible light irradiation at room temperature and atmospheric pressure. When these transition metal elements were added to a benchmark TiO<sub>2</sub> (commercial P25), the maximum hydrogen production efficiency was achieved for the Cu/TiO<sub>2</sub> photocatalyst, with ~5000 μmol h<sup>-1</sup> g<sup>-1</sup> and ~220 μmol h<sup>-1</sup> g<sup>-1</sup> H<sub>2</sub> production rates for UV and visible irradiation, respectively. These values were much higher than those obtained with the bare TiO<sub>2</sub> by factors of 16 and 3 for UV and visible light irradiation, respectively. Ni/TiO<sub>2</sub> and Co/TiO<sub>2</sub> also showed a significant photocatalytic activity when UV light was used. The best performing photocatalyst, Cu/TiO<sub>2</sub>, was further investigated by varying the copper amount from 0.1 to 9.0 wt% to identify the optimal cocatalyst loading. Two selected samples, containing 2.0 and 9.0 wt% of copper, were characterized by TEM and XPS. The results showed that Cu was highly dispersed over the TiO<sub>2</sub> support and Cu species existed as both reduced Cu<sup>0</sup>/Cu<sup>+</sup> and oxidized Cu<sup>2+</sup> on the surface of the titania matrix. Besides, during the hydrogen production reaction the ratio of the reduced to oxidized Cu decreased, most probably due to the transfer of photogenerated holes under UV or visible light. In the case of 2 wt% Cu/TiO<sub>2</sub> sample, both the optical properties, studied by photoluminescence, and the structural-chemical properties contribute to enhance the photocatalytic activity. A comparison was made with a Pt/TiO<sub>2</sub> system, which is considered by far the most efficient cocatalyst on TiO<sub>2</sub> for photocatalytic hydrogen production. However, it is worth noting that Cu/TiO<sub>2</sub> achieved ~80% of the H<sub>2</sub> production rate of Pt/TiO<sub>2</sub>, suggesting the great potential of such a photocatalyst as a very promising low cost alternative to Pt-based systems for hydrogen production.

## Conflicts of interest

There are no conflicts to declare.

## Acknowledgements

The authors would like to thank Ministerio de Economía y Competitividad of Spain (CTQ2015-68951-C3-3-R and MAT2016-80933-R), Ministerio de Ciencia, Innovación y

Universidades of Spain (Project RTI2018-099668-B-C22) and FEDER funds.

## Notes and references

- 1 I. Dincer and C. Acar, Review and evaluation of hydrogen production methods for better sustainability, *Int. J. Hydrogen Energy*, 2015, **40**, 11094.
- 2 F. Yilmaz, M. Tolga Balta and R. Selbaş, A review of solar based hydrogen production methods, *Renewable Sustainable Energy Rev.*, 2016, **56**, 171.
- 3 H. Caliskan, I. Dincer and A. Hepbasli, Exergoeconomic and environmental impact analyses of a renewable energy based hydrogen production system, *Int. J. Hydrogen Energy*, 2013, **38**, 6104.
- 4 I. Dincer, Exergetic and Sustainability Aspects of Green Energy Systems, *Clean: Soil, Air, Water*, 2007, **35**, 311.
- 5 J. D. Holladay, J. Hu, D. L. King and Y. Wang, An Overview of Hydrogen Production Technologies, *Catal. Today*, 2009, **139**, 244.
- 6 S. E. Hosseini and M. A. Wahid, Hydrogen production from renewable and sustainable energy resources: Promising green energy carrier for clean development, *Renewable Sustainable Energy Rev.*, 2016, **57**, 850–866.
- 7 S. Kitano, A. Tanaka, K. Hashimoto and H. Kominami, Metal ion-modified TiO<sub>2</sub> photocatalysts having controllable oxidative performance under irradiation of visible light, *Appl. Catal., A*, 2016, **521**, 202.
- 8 K. Chang, H. Xiao and Y. Jinhua, Transition Metal Disulfides as Noble-Metal-Alternative Co-Catalysts for Solar Hydrogen Production, *Adv. Energy Mater.*, 2016, **6**, 1502555.
- 9 Q. Jin, M. Fujishima, A. Iwaszuk, M. Nolan and H. Tada, Loading Effect in Copper(II) Oxide Cluster-Surface-Modified Titanium(IV) Oxide on Visible- and UV-Light Activities, *J. Phys. Chem. C*, 2013, **117**, 23848.
- 10 Q. Jin, H. Yamamoto, K. Yamamoto, M. Fujishima and H. Tada, Simultaneous induction of high level thermal and visible-light catalytic activities to titanium(iv) oxide by surface modification with cobalt(iii) oxide clusters, *Phys. Chem. Chem. Phys.*, 2013, **15**, 20313.
- 11 O. Kerkez-Kuyumcu, E. Kibar, K. Dayioglu, F. Gedic, A. N. Akın and S. Özkara-Aydinoglu, A comparative study for removal of different dyes over M/TiO<sub>2</sub> (M = Cu, Ni, Co, Fe, Mn and Cr) photocatalysts under visible light irradiation, *J. Photochem. Photobiol., A*, 2015, **311**, 176.
- 12 T. Hisatomi, J. Kubota and K. Domen, Recent advances in semiconductors for photocatalytic and photoelectrochemical water splitting, *Chem. Soc. Rev.*, 2014, **43**, 7520.
- 13 Y. Yu, G. Chen, Y. Zhou and Z. Han, Recent advances in rare-earth elements modification of inorganic semiconductor-based photocatalysts for efficient solar energy conversion: A review, *J. Rare Earths*, 2015, **33**, 453.
- 14 M. Ni, M. K. H. Leung, D. Y. C. Leung and K. Sumathy, A review and recent developments in photocatalytic water-





- splitting using TiO<sub>2</sub> for hydrogen production, *Renewable Sustainable Energy Rev.*, 2007, **11**, 401.
- 15 Y. Tamaki, A. Furube, M. Murai, K. Hara, R. Katoh and M. Tachiya, Dynamics of efficient electron-hole separation in TiO<sub>2</sub> nanoparticles revealed by femtosecond transient absorption spectroscopy under the weak-excitation condition, *Phys. Chem. Chem. Phys.*, 2017, **9**, 1453.
  - 16 K. Shimura and H. Yoshida, Heterogeneous photocatalytic hydrogen production from water and biomass derivatives, *Energy Environ. Sci.*, 2011, **4**, 2467.
  - 17 G. Colón, Towards the hydrogen production by photocatalysis, *Appl. Catal., A*, 2016, **518**, 48.
  - 18 M. C. Wu, P. Y. Wu, T. H. Lin and T. F. Lin, *Appl. Surf. Sci.*, 2018, **430**, 390.
  - 19 A. T. Montoya and E. G. Gillan, Enhanced Photocatalytic Hydrogen Evolution from Transition-Metal Surface-Modified TiO<sub>2</sub>, *ACS Omega*, 2018, **3**, 2947.
  - 20 K. K. Mandari, J. Y. Do, S. V. P. Vattikuti, A. K. R. Police and M. Kang, Solar light response with noble metal-free highly active copper(II) phosphate/titanium dioxide nanoparticle/copper(II) oxide nanocomposites for photocatalytic hydrogen production, *J. Alloys Compd.*, 2018, **750**, 292.
  - 21 M. K. Kumar, J. Y. Do, P. A. K. Reddy and M. Kang, Natural solar light-driven preparation of plasmonic resonance-based alloy and core-shell catalyst for sustainable enhanced hydrogen production: Green approach and characterization, *Appl. Catal., B*, 2018, **231**, 137.
  - 22 S. Velázquez-Martínez, S. Silva-Martínez, C. A. Pineda-Arellano, A. Jiménez-González, I. Salgado-Tránsito, A. A. Morales-Pérez and M. I. Peña-Cruz, Modified sol-gel/hydrothermal method for the synthesis of micro-sized TiO<sub>2</sub> and iron-doped TiO<sub>2</sub>, its characterization and solar photocatalytic activity for an azo dye degradation, *J. Photochem. Photobiol., A*, 2018, **359**, 93.
  - 23 M. Hinojosa-Reyes, R. Camposeco-Solís, R. Zanella and V. Rodríguez González, Hydrogen production by tailoring the brookite and Cu<sub>2</sub>O ratio of sol-gel Cu-TiO<sub>2</sub> photocatalysts, *Chemosphere*, 2017, **184**, 992.
  - 24 Y. Liu, Z. Wang and W. Huang, Influences of TiO<sub>2</sub> phase structures on the structures and photocatalytic hydrogen production of CuO<sub>x</sub>/TiO<sub>2</sub> photocatalysts, *Appl. Surf. Sci.*, 2016, **389**, 760.
  - 25 Z. Wang, K. Teramura, T. Shishido and T. Tanaka, Characterization of Cu Nanoparticles on TiO<sub>2</sub> Photocatalysts Fabricated by Electroless Plating Method, *Top. Catal.*, 2014, **57**, 975.
  - 26 A. Kubacka, M. J. Muñoz-Batista, M. Fernández-García, S. Obregón and G. Colón, Evolution of H<sub>2</sub> photoproduction with Cu content on CuO<sub>x</sub>-TiO<sub>2</sub> composite catalysts prepared by a microemulsion method, *Appl. Catal., B*, 2015, **163**, 214.
  - 27 D. Ni, H. Shen, H. Li, Y. Ma and T. Zhai, Synthesis of high efficient Cu/TiO<sub>2</sub> photocatalysts by grinding and their size-dependent photocatalytic hydrogen production, *Appl. Surf. Sci.*, 2017, **409**, 241.
  - 28 J. J. Velázquez, R. Fernández-González, L. Díaz, E. Pulido Melián, V. D. Rodríguez and P. Núñez, Effect of reaction temperature and sacrificial agent on the photocatalytic H<sub>2</sub>-production of Pt-TiO<sub>2</sub>, *J. Alloys Compd.*, 2017, **721**, 405.
  - 29 A. L. Linsebigler, G. Lu and J. T. Yates, Photocatalysis on TiO<sub>2</sub> Surfaces: Principles, Mechanisms, and Selected Results, *Chem. Rev.*, 1995, **95**, 735.
  - 30 J. Si, L. Yu, Y. Wang, Z. Huang, K. Homewood and Y. Gao, Colour centre-controlled formation of stable sub-nanometer transition metal clusters on TiO<sub>2</sub> nanosheet for high efficient H<sub>2</sub> production, *Appl. Surf. Sci.*, 2020, **511**, 145577.
  - 31 P. D. Tran, L. F. Xi, S. K. Batabyal, L. H. Wong, J. Barber and J. S. Loo, Enhancing the photocatalytic efficiency of TiO<sub>2</sub> nanopowders for H<sub>2</sub> production by using non-noble transition metal co-catalysts, *Phys. Chem. Chem. Phys.*, 2012, **14**, 11596.
  - 32 J. Si, Y. Wang, X. Xia, S. Peng, S. Xiao, L. Zhu, Y. Bao, Z. Huang and Y. Gao, Novel quantum dot and nano-sheet TiO<sub>2</sub> (B) composite for enhanced photocatalytic H<sub>2</sub>-Production without Co-Catalyst, *J. Power Sources*, 2017, **360**, 353.
  - 33 J. Liu, G. Hodes, J. Yan and S. Liu, Metal-doped Mo<sub>2</sub>C (metal = Fe, Co, Ni, Cu) as catalysts on TiO<sub>2</sub> for photocatalytic hydrogen evolution in neutral solution, *Chin. J. Catal.*, 2021, **47**, 205.
  - 34 K. C. Christoforidis and P. Fornasiero, Photocatalytic Hydrogen Production: A Rift into the Future Energy Supply, *ChemCatChem*, 2017, **9**, 1523.
  - 35 G. D. Moon, J. B. Joo, I. Lee and Y. Yin, Decoration of size-tunable CuO nanodots on TiO<sub>2</sub> nanocrystals for noble metal-free photocatalytic H<sub>2</sub> production, *Nanoscale*, 2014, **6**, 12002.
  - 36 J. Yu, X. Zhao and Q. Zhao, Effect of surface structure on photocatalytic activity of TiO<sub>2</sub> thin films prepared by sol-gel method, *Thin Solid Films*, 2000, **379**, 7.
  - 37 P. Khemthong, P. Photai and N. Grisdanurak, Structural properties of CuO/TiO<sub>2</sub> nanorod in relation to their catalytic activity for simultaneous hydrogen production under solar light, *Int. J. Hydrogen Energy*, 2013, **38**, 15992.
  - 38 I. Rossetti, Hydrogen Production by Photoreforming of Renewable Substrates, *ISRN Chem. Eng.*, 2012, 964936.
  - 39 E. P. Melián, C. R. López, A. O. Méndez, O. G. Díaz, M. N. Suárez, J. M. Doña-Rodríguez, J. A. Navío and D. Fernández-Hevia, Hydrogen production using Pt-loaded TiO<sub>2</sub> photocatalysts, *Int. J. Hydrogen Energy*, 2013, **38**, 11737.
  - 40 M. C. Hidalgo, M. Maicu, J. A. Navío and G. Colón, Photocatalytic properties of surface modified platinised TiO<sub>2</sub>: Effects of particle size and structural composition, *Catal. Today*, 2007, **129**, 43.
  - 41 <https://www.lme.com/>.
  - 42 E. Guo and L. Yin, Nitrogen doped TiO<sub>2</sub>-Cu<sub>x</sub>O core-shell mesoporous spherical hybrids for high-performance dye-sensitized solar cells, *Phys. Chem. Chem. Phys.*, 2015, **17**, 563.
  - 43 S. Zhu, S. Liang, Y. Tong, X. An, J. Long, X. Fu and X. Wang, Photocatalytic reduction of CO<sub>2</sub> with H<sub>2</sub>O to CH<sub>4</sub>



- on Cu(I) supported TiO<sub>2</sub> nanosheets with defective {001} facets, *Phys. Chem. Chem. Phys.*, 2015, **17**, 976.
- 44 W. T. Chen, V. Jovic, D. S. Waterhouse, H. Idriss and G. I. N. Waterhouse, The role of CuO in promoting photocatalytic hydrogen production over TiO<sub>2</sub>, *Int. J. Hydrogen Energy*, 2013, **38**, 15036.
  - 45 J. L. Cao, G. S. Shao, T. Y. Ma, Y. Wang, T. Z. Ren, S. H. Wu and Z. Y. Yuan, Hierarchical meso-macroporous titania-supported CuO nanocatalysts: preparation, characterization and catalytic CO oxidation, *J. Mater. Sci.*, 2009, **44**, 6717.
  - 46 H. Tian, L. Hu, C. Zhang, W. Liu, Y. Huang, L. Mo, L. Guo, J. Sheng and S. Dai, Retarded Charge Recombination in Dye-Sensitized Nitrogen-Doped TiO<sub>2</sub> Solar Cells, *J. Phys. Chem. C*, 2010, **114**, 1627.
  - 47 M. Jung, J. N. Hart, J. Scott, Y. H. Ng, Y. Jiang and R. Amal, Exploring Cu oxidation state on TiO<sub>2</sub> and its transformation during photocatalytic hydrogen evolution, *Appl. Catal., A*, 2016, **521**, 190.
  - 48 J. Yu, Y. Hai and M. Jaroniec, Photocatalytic hydrogen production over CuO-modified titania, *J. Colloid Interface Sci.*, 2011, **357**, 223.
  - 49 D. P. Kumar, N. L. Reddy, B. Srinivas, V. Durgakumari, V. Roddatis, O. Bondarchuk, M. Karthik, Y. Ikuma and M. V. Shankar, Stable and active Cu<sub>x</sub>O/TiO<sub>2</sub> nanostructured catalyst for proficient hydrogen production under solar light irradiation, *Sol. Energy Mater. Sol. Cells*, 2016, **146**, 63.
  - 50 V. Subramanian, E. E. Wolf and P. V. Kamat, Catalysis with TiO<sub>2</sub>/Gold Nanocomposites. Effect of Metal Particle Size on the Fermi Level Equilibration, *J. Am. Chem. Soc.*, 2004, **126**, 4943.
  - 51 J. M. Valero, S. Obregón and G. Colón, Active Site Considerations on the Photocatalytic H<sub>2</sub> Evolution Performance of Cu-Doped TiO<sub>2</sub> Obtained by Different Doping Methods, *ACS Catal.*, 2014, **4**, 3320.
  - 52 K. Czelej, J. C. Colmenares, K. Jabłczyńska, K. Cwieka, Ł. Werner and L. Gradoń, Sustainable hydrogen production by plasmonic thermophotocatalysis, *Catal. Today*, 2021, DOI: 10.1016/j.cattod.2021.02.004.

